Phase behavior and interfacial properties of nonadditive mixtures of Onsager rods

Kostya Shundyak,[1] René van Roij,[1] and Paul van der Schoot[2]

[1] *Institute for Theoretical Physics, Utrecht University, Leuvenlaan 4, 3584 CE Utrecht, The Netherlands*

[2] *Eindhoven Polymer Laboratories, Eindhoven University of Technology, P.O. Box 513, 5600 MB Eindhoven, The Netherlands*

(Dated: October 4, 2004)

Within a second virial theory, we study bulk phase diagrams as well as the free planar isotropic-nematic interface of binary mixtures of nonadditive thin and thick hard rods. For species of the same type the excluded volume is determined only by the dimensions of the particles, whereas for dissimilar ones it is taken to be larger or smaller than that, giving rise to a nonadditivity that can be positive or negative. We argue that such a nonadditivity can result from modelling of soft interactions as effective hard-core interactions. The nonadditivity enhances or reduces the fractionation at isotropic-nematic (IN) coexistence and may induce or suppress a demixing of the high-density nematic phase into two nematic phases of different composition (N_1 and N_2), depending on whether the nonadditivity is positive or negative. The interfacial tension between co-existing isotropic and nematic phases show an increase with increasing fractionation at the IN interface, and complete wetting of the IN_2 interface by the N_1 phase upon approach of the triple point coexistence. In all explored cases bulk and interfacial properties of the nonadditive mixtures exhibit a striking and quite unexpected similarity with the properties of additive mixtures of different diameter ratio.

PACS numbers: 61.30.Cz, 61.30.Hn, 05.70.Np, 68.08.Bc

I. INTRODUCTION

In his paper about the isotropic-nematic (IN) transition in solutions of monodisperse, rod-like particles that interact through a hard, steric repulsion, Onsager briefly discussed a possible extension of his results to polydisperse systems[1]. Since then, a tremendous amount of work has been devoted to the study of the influence of polydispersity on the phase behavior of such hard-rod fluids, both for the case where this polydispersity is of the quenched type[2,3] and for where it is of the annealed type[4,5]. Focusing on the former, even the simplest (binary) mixtures consisting of long hard rods that differ only in length or diameter exhibit quite nontrivial phase diagrams. In addition to the pure isotropic and nematic phases of various composition and regions of their coexistence, the high-density nematic phase can demix (and possibly remix) into two nematic phases of different composition (denoted N_1 and N_2). The reason for the existence of an IN transition in binary mixtures is the same as that in a monodisperse hard-rod fluids, being a competition between orientation entropy and entropy of packing[1,6]. In contrast, the nematic-nematic demixing does not involve changes in excluded volume (i.e. packing entropy), but rather a competition between orientation entropy and entropy of mixing[7]. Another interesting feature is that for sufficiently large size disparity, the two distinct nematic phases do not remix even at arbitrary high pressure[9].

Unfortunately, it is quite difficult to compare these theoretical findings with results obtained from actual experiments. Although rod-like particles can be synthesized chemically in various ways[6], typically their size distribution is mono- or bi-disperse only to a first approximation. By contrast, suspensions of rod-like viruses such as tobacco mosaic virus, M13, pf1 and fd are characterized by a high degree of monodispersity, and are therefore attractive model systems, despite the complicating factors associated with their fixed physical dimensions, their charged nature and the fact that they are not actually infinitely rigid but exhibit some degree of bending flexibility.

Recently, however, experimental procedures have been developed that allow one to modify the length and the diameter of these viruses[10], which opens the possibility to form binary mixtures of a well-defined bidispersity. In particular, one of the methods is based on altering the effective diameter of the fd-virus by coating it with the polymer polyethylene glycol (PEG). Studies of such binary mixtures of thin and thick rods have revealed coexistence regions of the isotropic and different nematic phases (IN_2 and IN_1), as well as a nematic-nematic coexistence region (N_1N_2) and an IN_1N_2 triple point[11]. Although some of the gross features of this experimentally determined phase diagram are in agreement with theoretical predictions based on an extension of Onsager's second-virial theory to binary mixtures of hard rods[12,13], some of the experimental and theoretical findings turn out to be in sharp contrast with each other.

According to the theory, mixtures of thin rods (with a diameter D_1) and thick ones (diameter D_2) of equal length L should exhibit a spindle-like IN coexistence without any nematic-nematic demixing for diameter ratios $d = D_2/D_1 < 3.8$. Experiments, however, point at a broad N_1N_2 coexistence for a diameter ratio as small as $d \sim 2.0$[11]. Furthermore, in the interval $3.8 < d < 4.29$

the single nematic phase demixes according to the theory into two nematic phases N_1 and N_2 of different composition, whilst remixing takes place at sufficiently high total density (or osmotic pressure), that is, above an *upper* critical (or consolute) point. Experiments, however, reveal a *lower* consolute point that closes the $N_1 - N_2$ coexistence[11], i.e., the $N_1 - N_2$ demixing becomes more pronounced with increasing osmotic pressure.

Possible explanations for these differences may well be found in the idealisations incurred when modelling the virus particles as infinitely elongated, infinitely rigid rods that interact with each other only through additive hard-core potentials. Indeed, the virus particles are semi-flexible and charged, as already alluded to. In addition, the grafted polymer coating is soft and hence compressible, and the length-to-breath ratio of the rods is at best, say, 50. It is important to recall that the second virial theory is believed to be exact only in the limit of infinite aspect ratios of the rods[6]. The impact of a finite length-to-diameter ratio was recently considered within an extension of the so-called Parsons-Lee theory to mixtures of hard rods[14]. This theory does reproduce a lower consolute point for mixtures of thin and thick rods albeit only if their length (presumed equal) is extremely small. A lower consolute point has also been predicted for binary mixtures of semi-flexible hard thin rods of unequal thickness, at least if their persistence lengths and their widths do not differ by more than roughly the square root of either persistence length over their contour length[15,16]. However, the predicted isotropic-isotropic demixing is not found in the experiments involving the mixtures of naked and coated fd virus particles[11]. The theory[15,16] does anyway not strictly apply to this experimental system, because of the tacit assumption that the length of the rods greatly exceeds their persistence length.

In an attempt to shed light on the issue, we focus on the effects that any nonadditivity of the interactions between the two kinds of rod might have on their phase behavior. Such a nonadditivity emerges naturally if one replaces actual soft rod-rod repulsions by effective hard-core repulsions, characterized by effective hard-core diameters that in effect are distances of closest approach. As is well known, the screened-Coulomb interactions between charged virus particles in an electrolyte solution can be reasonably approximated by an effective steric interaction with a hard-core diameter that is the sum of the bare, "physical" diameter of the rod and an electrostatic contribution proportional to the Debye screening length of the suspending medium[17]. For the interaction between a pair of polymer-coated virus particles one would have an effective diameter of the order of the radius of gyration of the tethered chains[8], at least if the Debye length is much smaller than that.

It is not at all obvious that the effective interaction length between a bare and a polymer-coated charged rod should be the linear average of the interaction lengths of the two separate species, in other words, one would from the outset expect the interaction within such an effective description to be non-additive rather than additive. Indeed, as we shall see below in section II, even highly simplified model potentials produce non-additive effective hard-core interactions in mixtures of rods. The level of nonadditivity may be expressed in a parameter α defined such that the effective hard-core diameter of an unlike pair of rods can written as $\frac{1}{2}(D_1 + D_2)(1 + \alpha)$, where D_σ is the effective hard-core diameter of the interaction between two like rods of species $\sigma = 1, 2$. For an additive mixute, $\alpha = 0$. In this paper, we make plausible by explicitly considering the steric interactions between the various types of rod that, even within a simplified model, α may attain values that can be positive or negative up to, say, ten per cent. Additional sources of nonadditivity may be found, say, in electric polarisation effects of the charges on the polymer coating, but these will not be considered here.

Although the microscopic origin of nonadditivity is ultimately based on the less ($\alpha > 0$) or more ($\alpha < 0$) efficient packing of the mixture compared to the pure species, we do not attempt to calculate α from a realistic microscopic theory. Having ascertained that α need indeed not be zero, we treat it as a phenomenological parameter in a generalised Onsager theory, and investigate its consequences for the phase behavior of the mixture, and for the interfacial properties of co-existing isotropic and nematic phases. As we shall see, both the predicted phase diagrams and interfacial properties of the isotropic-nematic interface are very sensitive to values of $|\alpha|$ as small as a few per cent. Of course, this does not imply that all effects of electrostatic interactions, flexibility, etc., are accurately or even properly modelled. In fact, we find that non-additivity cannot explain the existence of the lower consolute point found by Fraden and co-workers[11].

The remainder of this paper is organized as follows. In Sec. II we introduce a simple model for polymer-coated rods, and provide an estimate for typical values of the nonadditivity parameter α. In Sec. III we introduce the Onsager-type free energy functional, and derive from that the basic Euler-Lagrange equations describing the orientational and density distribution of the rods under conditions of thermodynamic equilibrium. In Sec. IV we solve these equations for bulk geometries, and analyze the structure of a few typical bulk phase diagrams. In Sec. V we briefly describe a method to solve the Euler-Lagrange equation for interface geometries of binary mixtures, and study IN_1, N_1N_2 and IN_2 interfaces, the latter in particular in the vicinity of the bulk IN_1N_2 triple point. A summary and discussion of the results are presented in Sec. VI.

II. NONADDITIVITY OF INTERACTIONS

The physical origin of nonadditivity can be illustrated on the basis of a simple model for a mixture of bare and PEG-coated fd viruses[11]. The bare rods are modelled

as rigid hard rods of length L and diameter Δ_1 ($L \gg \Delta_1$), and hence the interaction potential between two bare rods, $\phi_{11}(r)$, is given by $\beta\phi_{11}(r) = \infty, 0$ for $r < \Delta_1$ and $r > \Delta_1$, respectively. Here, r denotes the shortest distance between the main axes of the two rods.

The PEG-coated rods are identical to the bare ones, except that they bear an additional soft layer extending to a distance $\Delta_2/2$ from the axis of the rod, i.e., to a distance $(\Delta_2 - \Delta_1)/2$ from their hard-core surface. We do not specify the relation between the dimensions of the tethered PEGs and Δ_2 in any detail, but one expects that $(\Delta_2 - \Delta_1)/2$ is of the order of the radius of gyration of the grafted PEG (so we only consider $\Delta_2 > \Delta_1$). We expect that the soft, repulsive interaction that occurs when the polymer coating of two rods overlap should be quite similar to that of overlapping star polymers[18]. In order to keep the model as simple as possible, we represent the interaction of mean force resulting from the presence of a polymer coating by a square-shoulder potential that is a function of r alone, and ignore any angle dependence that might arise in reality. This angular dependence should be significant only for configurations of rods inclined at small angles, which bear only a tiny statistical weight in the limit of large aspect ratios. Note that although our representation of the soft potential is isotropic, the virials based on it are anisotropic because the interaction volumes are a function of the relative orientations of the rods.

The interaction potential between a bare and a coated rod, $\phi_{12}(r)$, should obviously be identical to the naked-rod potential $\phi_{11}(r)$ if $r < \Delta_1$ and $r > (\Delta_2 + \Delta_1)/2$. Within our description, $\phi_{12}(r)$ takes on a value different from that, $\epsilon_1 > 0$, if $\Delta_1 < r < (\Delta_1 + \Delta_2)/2$, i.e., when the hard-core of the bare rod perturbes the soft outer layer of the coated rod. It is to be seen as an average of the actual interaction potential over its range. Our effective interaction potential between two coated rods, $\phi_{22}(r)$, is more complicated and consists of two shoulders in between the range of the hard-core repulsion ($r < \Delta_1$) and the noninteracting long-distance regime ($r > \Delta_2$). The first shoulder, for $\Delta_1 < r < (\Delta_1 + \Delta_2)/2$, is such that $\phi_{22}(r) = 2\epsilon_1$, and represents the overlap of the hard core of the first rod with the polymer layer of the second one, and *vice versa* by symmetry. The second shoulder, for $(\Delta_1 + \Delta_2)/2 < r < \Delta_2$, represents overlap of the two polymer layers, and is such that $\phi_{22}(r) = \epsilon_2 > 0$.

The nature of the polymer chains is such that we expect their entropy to be reduced more by a penetrating rigid rod than by another polymer. Indeed, the cross virial of a rod and a flexible chain is much larger than the geometric average of the rod-rod and the chain-chain virials[19]. For this reason we only consider cases where $2\epsilon_1 > \epsilon_2$. The pair potentials $\phi_{\sigma\sigma'}(r)$ between rods of species σ and σ' are illustrated graphically in Fig. 1.

It is a straightforward exercise to calculate the second virial coefficients $B_{\sigma\sigma'}$ averaged over all angles, from the pair interactions $\phi_{\sigma\sigma'}(r)$ given above[1,6]. In the Onsager limit $L \gg \Delta_2 \geq \Delta_1$, where terms of order $L\Delta^2$ can be ignored, one finds

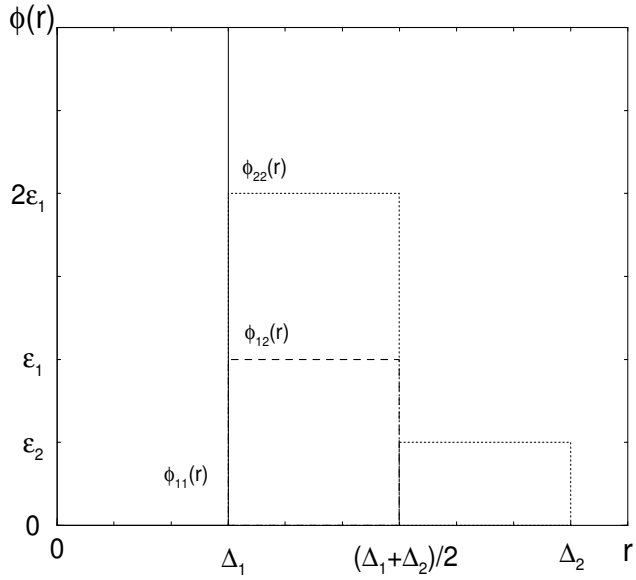

FIG. 1: Interaction potentials $\phi_{11}(r)$, $\phi_{12}(r)$, $\phi_{22}(r)$ between bare-bare (solid), bare-coated (dashed), coated-coated (dotted line) rods, respectively, as a function of the (shortest) distance r between the axes of the two rods.

$$B_{11} = (\pi/4)L^2\Delta_1, \tag{1}$$

$$B_{12} = (\pi/4)L^2\left(\Delta_1 + \frac{\Delta_2 - \Delta_1}{2}\left(1 - e^{-\beta\epsilon_1}\right)\right), \tag{2}$$

$$B_{22} = (\pi/4)L^2\left(\Delta_1 + \frac{\Delta_2 - \Delta_1}{2}\left(2 - e^{-2\beta\epsilon_1} - e^{-\beta\epsilon_2}\right)\right). \tag{3}$$

These expressions can be used to map the model mixture of bare and PEG-coated rods onto a mixture of hard rods with effective hard-core diameters D_1 and D_2. We choose D_1 and D_2 to be such that the like-like second virial coefficients of the effective hard-core system are identical to B_{11} and B_{22} given in Eq. (1) and (3), respectively, i.e., we impose that $B_{\sigma\sigma} = (\pi/4)L^2D_\sigma$. This yields

$$\begin{aligned} D_1 &= \Delta_1 \\ D_2 &= \Delta_1 + \frac{\Delta_2 - \Delta_1}{2}(2 - \exp(-2\beta\epsilon_1) - \exp(-\beta\epsilon_2)). \end{aligned} \tag{4}$$

One may verify that $D_2 = \Delta_2$ in the limit that $\beta\epsilon_i \to \infty$, as expected. We now also impose that the cross virial coefficient of the effective hard-core system equals B_{12} given in Eq. (2). For arbitrary ϵ_1 and ϵ_2 this requires a nonadditivity parameter α such that $B_{12} = (\pi/8)L^2(D_1 + D_2)(1 + \alpha)$, which yields

$$\alpha = \frac{1}{d+1}\left[2 + \frac{2(d-1)(1 - \exp(-\beta\epsilon_1))}{2 - \exp(-2\beta\epsilon_1) - \exp(-\beta\epsilon_2)}\right] - 1, \tag{5}$$

with $d = D_2/D_1$ the effective diameter ratio of the rods. In Fig. 2 we show the contour plot of the nonadditivity parameter α as a function of the energy scales ϵ_1

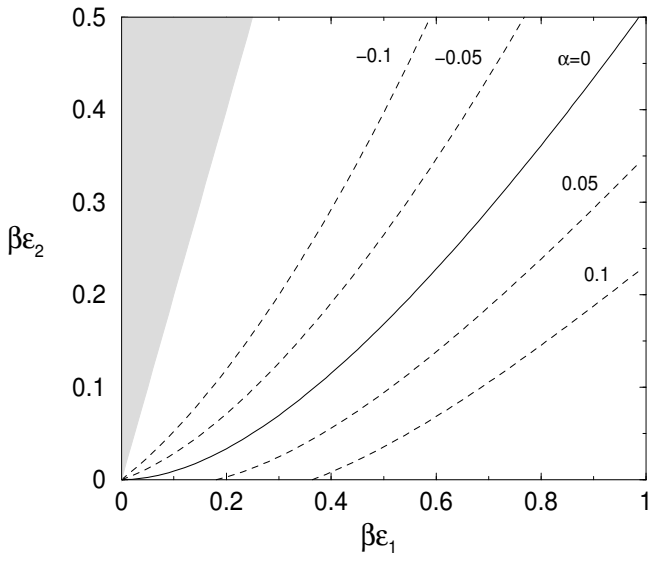

FIG. 2: Contour plot of the nonadditivity parameter α as a function of the square-shoulder values ϵ_1 and ϵ_2 for the effective diameter ratio $D_2/D_1 = d = 3.5$. The grey area denotes the nonphysical region $\epsilon_2 > 2\epsilon_1$ (see text).

and ϵ_2 for the effective diameter ratio $d = 3.5$, which is the value that we will use in our calculations below; other values for d produce similar contour plots. The grey area in Fig. 2 is the regime deemed unphysical, with $2\epsilon_1 < \epsilon_2$. As one can see, for physically reasonable values of ϵ_1 and ϵ_2 of the order of k_BT both positive and negative values for α are possible, even when $\epsilon_1 > \epsilon_2$. The crossover from positive to negative nonadditivity takes place, independently from the value of d, when $\exp(-\beta\epsilon_2) = 2\exp(-\beta\epsilon_1) - \exp(-2\beta\epsilon_1)$, i.e., when $\beta\epsilon_2 \sim (\beta\epsilon_1)^2$ if $\beta\epsilon_1 < 1$ and $\beta\epsilon_2 \sim \beta\epsilon_1 - \ln 2$ if $\beta\epsilon_1 > 1$. Presuming that both $\beta\epsilon_1$ and $\beta\epsilon_2$ are indeed of the order unity, we expect $|\alpha|$ to be in the range $10^{-2} - 10^{-1}$. Such small deviations from additivity are sufficient to qualitatively alter the phase behavior of the rods, as we shall see next. In our study, we from now on treat α, D_1 and D_2 as independent parameters. We investigate both the bulk and the interfacial behavior of the effectively purely hard-core system, in which the soft interactions are incorporated through the degree of non-additivity α.

III. DENSITY FUNCTIONAL AND METHOD

Consider a fluid of hard cylinders of two different species $\sigma = 1, 2$ of diameter D_σ and equal length L ($D_\sigma/L \to 0$) in a macroscopic volume V at temperature T and chemical potentials μ_σ. Let $\mathbf{r}$ denotes the center-of-mass coordinate of a rod and $\hat{\omega}$ the orientation of the long axis. The interactions between the $\sigma\sigma'$-pair of rods with coordinates $q = \{\mathbf{r}, \hat{\omega}\}$ and $q' = \{\mathbf{r}', \hat{\omega}'\}$ are characterized by a hard-core potential, which is the simple contact potential for rods of the same species ($\sigma = \sigma'$), whereas for unlike rods ($\sigma \neq \sigma'$) it corresponds to interactions between hard rods of diameter $(1+\alpha)D_1$ and $(1+\alpha)D_2$.

Within the second virial approximation and in the absence of external potentials, the grand potential functional $\Omega[\{\rho_\sigma\}]$ of the one-particle distribution functions $\rho_\sigma(\mathbf{r}, \hat{\omega})$ can be written[1,6,13] as

$$\beta\Omega[\{\rho_\sigma\}] = \sum_\sigma \int dq \rho_\sigma(q) \Big(\ln[\rho_\sigma(q) L^2 D_\sigma] - 1 - \beta\mu_\sigma \Big) - \frac{1}{2} \sum_{\sigma\sigma'} \int dq dq' f_{\sigma\sigma'}(q;q') \rho_\sigma(q) \rho_{\sigma'}(q'), \quad (6)$$

with $\beta = (k_BT)^{-1}$ the inverse temperature, and $f_{\sigma\sigma'}(q, q')$ the Mayer function, which equals -1 if the rods overlap and vanishes otherwise. Since we consider the limit $D_\sigma/L \to 0$ for any σ, the relative shape disparity of rods is characterized by the ratio $d = D_2/D_1$ of the diameters and the value of the nonadditivity α.

The minimum conditions $\delta\Omega[\{\rho_\sigma\}]/\delta\rho_\sigma(q) = 0$ on the functional lead to the set of nonlinear integral equations

$$\ln[\rho_\sigma(q) L_\sigma^2 D_\sigma] - \sum_{\sigma'} \int dq' f_{\sigma\sigma'}(q;q') \rho_{\sigma'}(q') = \beta\mu_\sigma \quad (7)$$

to be solved for the equilibrium distributions $\rho_\sigma(q)$. These equations are identical to the Euler-Lagrange equations for additive rods mixtures, and we can directly apply the method developed earlier[12,13]. The structure of the bulk phase diagram depends now on the value of the nonadditivity parameter α, and has to be determined first.

Since the bulk distribution functions of the isotropic and nematic phase are translationally invariant, i.e., $\rho_\sigma(\mathbf{r}, \hat{\omega}) = \rho_\sigma(\hat{\omega})$, we can reduce Eq. (7) to

$$\ln[\rho_\sigma(\hat{\omega}) L_\sigma^2 D_\sigma] + \sum_{\sigma'} \int d\hat{\omega}' E_{\sigma\sigma'}(\hat{\omega}, \hat{\omega}') \rho_{\sigma'}(\hat{\omega}') = \beta\mu_\sigma, \quad (8)$$

with $E_{\sigma\sigma'}$ the excluded volume of a pair of cylinders of species σ and σ' given by

$$E_{\sigma\sigma'}(\hat{\omega}, \hat{\omega}') = -\int d\mathbf{r}' f_{\sigma\sigma'}(\mathbf{r}, \hat{\omega}; \mathbf{r}', \hat{\omega}') = L^2 (D_\sigma + D_{\sigma'})(1 + \alpha(1 - \delta_{\sigma,\sigma'})) |\sin\varphi| \quad (9)$$

in terms of the angle φ between $\hat{\omega}$ and $\hat{\omega}'$, i.e., $\varphi = \arccos(\hat{\omega} \cdot \hat{\omega}')$. Note that additional $O(LD^2)$ terms are being ignored in Eq. (9), in line with the needle limit ($D_\sigma/L \to 0$) of interest here. Given the linear dependence of the excluded volume on D_σ, one can see that

$$E_{12}(\hat{\omega}, \hat{\omega}') = \frac{1}{2}(E_{11}(\hat{\omega}, \hat{\omega}') + E_{22}(\hat{\omega}, \hat{\omega}'))(1 + \alpha). \quad (10)$$

In some sense, α plays a similar role in the present context as the so-called χ -parameter in the Flory theory of polymer solutions on a lattice, where demixing is driven by

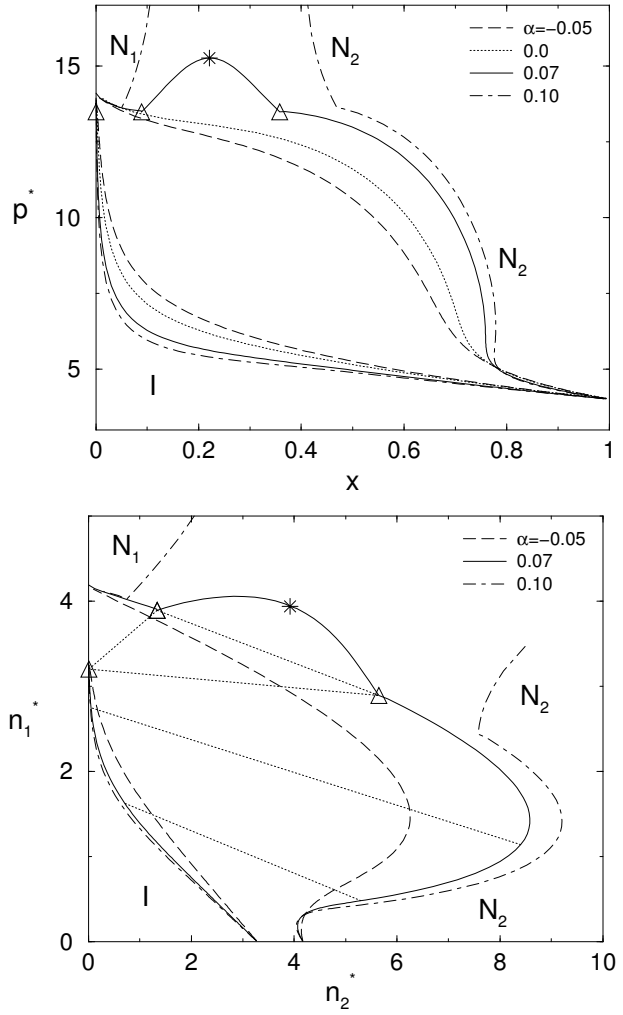

FIG. 3: (a) Bulk phase diagrams of binary thin-thick mixtures (diameter ratio $d = 3.5$) for different nonadditivity parameter α in the $p - x$ representation, with $p^* = (\pi/4)\beta p L^2 D_1$ the dimensionless pressure, and x the mole fraction of the thicker rods. We distinguish the fully symmetric isotropic phase (I) and orientationally ordered nematic phases (N_1 and N_2). For the nonadditivity parameter $\alpha = 0.07$ the IN_1N_2 triple phase coexistence is marked by ($\triangle$), and the N_1N_2 critical point by ($*$). (b) The same phase diagrams in density-density representation, where $n_1^* = n_1 L D_1^2(\pi/4)$ and $n_2^* = n_2 L D_2^2(\pi/4)$ are the dimensionless bulk number densities of thin and thick rods, respectively. The tie-lines connect coexisting state points.

direct unfavorable nearest neighbor interaction between unlike species as compared to that between like species.

Details of the numerical schemes to solve Eq. (8) have been discussed elsewhere[12,13]. Here we use a nonequidistant θ-grid of $N_\theta = 30$ points $\theta_i \in [0, \pi/2]$, where $1 \leq i \leq N_\theta$, in order to find the bulk distributions $\rho_\sigma(\theta_i)$. Coexistence of different phases $\{I, N_1, N_2\}$ is determined by imposing conditions of mechanical and chemical equilibrium.

IV. BULK PHASE DIAGRAMS

In Fig. 3 we show both pressure-composition (a) and density-density (b) representations of bulk phase diagrams of thin-thick binary mixtures ($L_\sigma = L, D_2 > D_1$) for the diameter ratio $d = 3.5$ at various values of the nonadditivity parameter α. In Fig. 3(a) the composition variable $x = n_2/(n_1 + n_2)$ denotes the mole fraction of thick rods, $n_\sigma = \int d\hat{\omega} \rho_\sigma(\hat{\omega})$ is the number density of species σ, and $p^* = (\pi/4)\beta p L^2 D_1$ is a dimensionless bulk pressure. Note that the IN coexistence pressure p_{thin} and p_{thick} of the pure thin ($x = 0$) and pure thick ($x = 1$) system are given by $(\pi/4)\beta p_{thin} L^2 D_1 = (\pi/4)\beta p_{thick} L^2 D_2 = 14.045$, i.e., $p_{thick} = p_{thin}/d$, and that the tie-lines connecting coexisting phases are horizontal in the $p - x$ representation of Fig. 3(a). This representation is convenient for theoretical analysis, whereas the densities (volume fractions) of thin and thick rods are experimental control parameters[20]. For this reason the same phase diagrams of thin-thick binary mixtures are shown in Fig. 3(b) in the density-density representation, with $n_1^* = n_1 L D_1^2(\pi/4)$ and $n_2^* = n_1 L D_2^2(\pi/4)$ being the dimensionless bulk number densities of thin and thick rods, respectively. In this representation the tie-lines, indicated by the dotted lines, are no longer horizontal.

The structures of the bulk phase diagrams for various α show a striking similarity with the bulk phase diagrams of additive binary mixtures of thin and thick hard rods[13]. At low pressures (or low densities) the phase diagrams show an isotropic (I) phase, and at higher pressures (or densities) one ($\alpha < 0.07$) or two ($\alpha \geq 0.07$) nematic phases (N_1 and N_2). For $\alpha < 0.07$ the phase diagram is spindle-like, and the only feature is a strong fractionation at coexistence, such that the nematic phase is relatively rich in thick rods and the isotropic phase in thin ones. Although the nonadditivity modifies the fractionation gap, the reason behind it remains the same: the relatively large excluded volume in interactions of the thick rods makes them more susceptible to orientational ordering[12,21,22]. As a general tendency, the fractionation at isotropic-nematic coexistence becomes stronger for increasing values of α.

For $\alpha > 0.06$ the bulk phase diagram develops nematic-nematic (N_1N_2) coexistence in a pressure regime $p > p_t$, with p_t the triple-point pressure. Using the simple Gaussian ansatz for one-particle distribution functions, one can demonstrate that the packing entropy does not play a role in nematic demixing in our system, similar to the case of additive mixtures[7]. Although it is known that the functional form of $\rho_\sigma(\hat{\omega})$ is not Gaussian even at high densities, an analysis of the exact high-density distribution functions confirmed such a mechanism of nematic demixing[12]. On this basis we assume it to be valid at arbitrary high pressure in our system, and expect the structure of the bulk phase diagrams to be similar to those of additive mixtures. In particular, for $\alpha = 0.07$ nematic remixing is observed at a sufficiently high pressure, as illustrated in Fig. 3. The consolute point, at

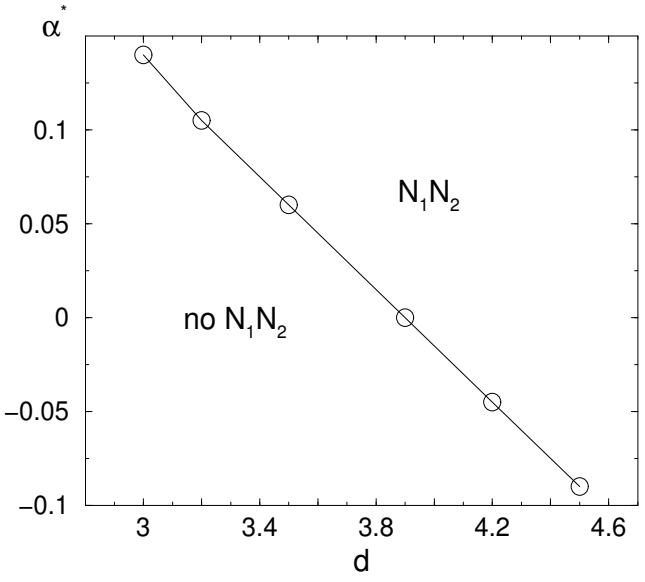

FIG. 4: Nonadditivity parameter α^* at which the consolute point and triple point coincide for various values of the diameter ratio d. For mixtures, characterized by $\alpha(d) < \alpha^*(d)$ the N_1N_2 demixing is not detected.

which the density and composition difference between the coexisting nematic phases vanishes, is indicated by $(*)$. For $\alpha = 0.1$, limitations of the numerical scheme[23] do not allow us to determine whether or not remixing takes place at high enough pressures. We note that in the limit of very high pressures, where the rods increasingly align themselves, both end corrections and higher order virials need to be taken into account for an accurate description of the phase behavior. On the other hand, in analogy with additive mixtures, one expects that critical values of α and d, beyond which the nematic does not take place at arbitrary high densities, exist[12].

In order to characterize the amount of nonadditivity in the excluded volume interactions which leads to significant structural modification of the phase diagram (i.e. nematic demixing), we explore various thin-thick mixtures of different values of α and d, and determine the value of α^* for which the pressure of the nematic-nematic consolute point and the triple point pressure coincide. Results of our studies are presented in Fig. 4. For $\alpha < \alpha^*$ (at fixed d) the N_1N_2 phase separation is not detected, and for $\alpha \geq \alpha^*$ there is N_1N_2 coexistence in the phase diagram. It is evident that in the interval $d \in [3.5, 4.2]$ even a small nonadditivity $|\alpha| < 5 - 7\%$ may induce or suppress the N_1N_2 demixing transition.

One might surmise that the linearity of the function $\alpha^*(d)$ within the explored range of α reflects the linearity of the excluded volume $E_{12}(\hat{\omega}, \hat{\omega}')$ in terms of d and α, because it drives the nematic-nematic phase separation. The mapping of the non-additive to the additive case is not trivial, however, for the data of Fig. 4 do not quite obey the relation $d + \alpha d + \alpha \to d$ that one would naively expect from Eq. (9). Nonetheless, direct comparison of the bulk phase diagrams of the nonadditive mixture with $d = 3.5$ and $\alpha = 0.07$ and the additive mixture with $d = 4.0$ (presented in[13]) shows close values of the fractionation gap at the N_1N_2 coexistence. Further evidence for similarity of these systems in the high density regime will be demonstrated in our analysis of their interfacial properties presented next.

V. INTERFACES

Free planar interfaces between various coexisting bulk phases can be studied similar to the interfaces of additive mixtures[13,24,25]. We focus on the nonadditive thin-thick mixture characterized by $d = 3.5$ and $\alpha = 0.07$. The nematic director $\hat{n}$ of the asymptotic nematic bulk phase(s) can, in general, have a nontrivial tilt angle $\theta_t = \arccos(\hat{n} \cdot \hat{z})$ with respect to the interface normal. In the present calculations we restrict attention to $\theta_t = \pi/2$, i.e., $\hat{n} \perp \hat{z}$. As we have checked, this geometry is thermodynamically favorable because of its minimal surface tension.

Similar to the studies of additive mixtures, we use the planar symmetry of the interfaces and assume the distribution functions to be uniaxially symmetric with respect to the director, i.e. $\rho_\sigma(\mathbf{r}, \hat{\omega}) = \rho_\sigma(z, \theta)$, which reduce Eqs. (7) to

$$\beta\mu_\sigma = \ln[\rho_\sigma(z,\theta) L_\sigma^2 D_\sigma] + \sum_{\sigma'} \int dz' d\theta' \sin\theta' \times \mathcal{K}_{\sigma\sigma'}(z - z', \theta, \theta') \rho_{\sigma'}(z', \theta'), \quad (11)$$

with $\mathcal{K}_{\sigma\sigma'}(z - z', \theta, \theta') = -\frac{1}{2\pi} \int d\varphi d\varphi' dx' dy' f_{\sigma\sigma'}(q, q')$. We solve Eq. (11) in order to determine uniaxially symmetric nonuniform distributions $\rho_\sigma(z, \theta_i)$ using an equidistant z-grid of $N_z = 200$ points in the interval $z \in [-5L, 5L]$, and corresponding bulk distributions $\rho_\sigma(\theta_i)$ as boundary conditions. Further details of the numerical calculations were discussed in Ref.[13].

The IN_1 and N_1N_2 interfaces are found to be smooth and monotonic, in the sense that the profiles of the nematic uniaxial order parameters $S_\sigma(z)$ and the densities $n_\sigma(z)$ change monotonically from the bulk values in the I (N_1) phase to those in the N_1 (N_2) phase. The correlation length ξ_{N_1} of the bulk N_1 phase at the triple-phase coexistence (as well as ξ_I and ξ_{N_2} for the I phase and the N_2 phase, respectively) can be extracted from the asymptotic decay of the one-particle distributions $\rho_\sigma(z, \theta)$ to their bulk values $\rho_\sigma^{N_1}(\hat{\omega})$, since the deviation $\delta\rho_\sigma(z, \hat{\omega}) = \rho_\sigma(z, \hat{\omega}) - \rho_\sigma^{N_1}(\hat{\omega})$ is of the form[13]

$$\delta\rho_\sigma(z, \hat{\omega}) = A_\sigma(\hat{\omega}) \exp(-z/\xi_{N_1}), \quad z \to \infty. \quad (12)$$

Interestingly, we find that $\xi_{N_1}/L = 0.49 \pm 0.02$ is the same as for the additive mixture with $d = 4.0$[13], which has a virtually identical phase diagram.

The properties of the IN_2 interfaces depend strongly on the pressure difference with the triple point (IN_1N_2

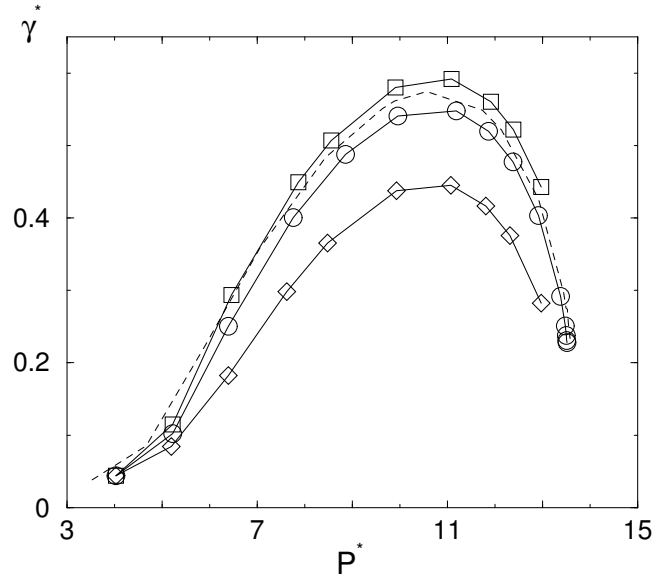

FIG. 5: Dimensionless surface tension $\gamma^*_{IN_2} = \beta\gamma_{IN_2}LD_1$ of IN_2 interfaces as a function of dimensionless pressure $p^* = \beta pL^2D_1(\pi/4)$ for thin-thick mixtures with diameter ratio $d = 3.5$ and different values of nonadditivity $\alpha = 0.0$ ($\diamond$), 0.07 ($\circ$) and 0.1($\square$). The dashed line indicates $\gamma^*_{IN_2}(p^*)$ for the additive thin-thick mixture of diameter ratio $d = 4.0$.

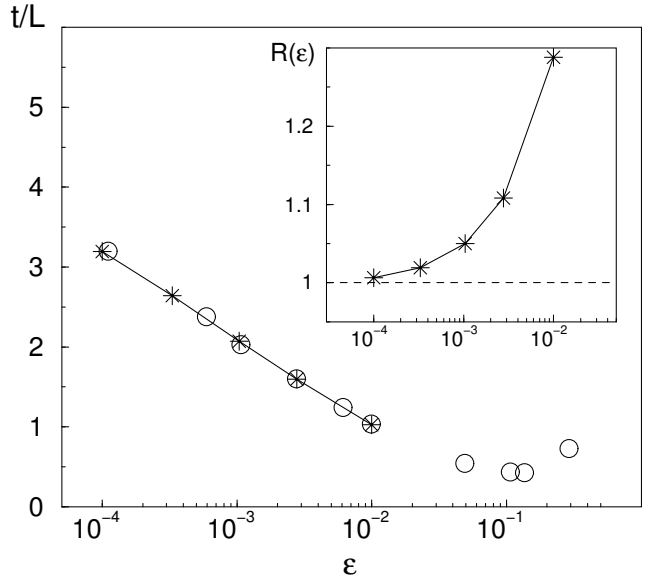

FIG. 6: Thickness t/L as a function of the undersaturation $\epsilon = 1 - p/p_t$ from the triple point pressure p_t for thin-thick mixtures with diameter ratio $d = 3.5$ and nonadditivity $\alpha = 0.07$ ($*$). For comparison we show thickness of the IN_2 interface of the additive mixtures for $d = 4.0$ ($\circ$). The inset shows the surface tension ratio R [see Eq. (13)] as a function of the triple point undersaturation ϵ.

phase coexistence). As it is demonstrated in Fig. 5, the surface tension of the IN_2 interface shows a non-monotonic dependence on the bulk pressure p, and strongly correlated with the fractionation at the IN_2 coexistence. Upon increasing the nonadditivity, the surface tension $\gamma^*_{IN_2}(p)$ grows, again indicating that α plays a role similar to the diameter ratio d. For comparison we have included $\gamma^*_{IN_2}(p)$ for an additive thin-thick mixture with $d = 4.0$, which is again quite close to the results for the nonadditive mixtures with $d = 3.5$ and $\alpha = 0.07$ and 0.1.

The microscopic thickness t of the interface is defined as $t = |z_+ - z_-|$ where $z_\pm$ are solutions of ${n_1}'''(z) = 0$, and a prime denotes differentiation with respect to z. As this equation has a set of solutions in every interfacial region, we choose for $z_\pm$ the outermost ones, i.e., the ones nearest to the bulk phases. The density of thin rods is a convenient representation of structural changes within the interface, since they have a smaller excluded volume and a non-vanishing concentration in both coexisting phases. This criterion provides a single measure for the thickness of both monotonic and non-monotonic profiles, with and without a thick film in between the asymptotic bulk phases at $z \to \pm\infty$. The interfacial width for the one-component IN interface is, with the present definition, given by $t/L = 0.697$.

The thickness of the IN_2 interface was found to diverge upon approach of the triple-point pressure p_t. This can be seen in Fig. 6, where t/L is plotted as a function of the dimensionless undersaturation $\epsilon = 1 - p/p_t$, which is a convenient measure of the pressure difference with the triple point. The nature of the film can be analyzed from the density profiles $n_1(z)$ of the IN_2 interface (or equivalently $S_\sigma(z)$, or $n_2(z)$). In Fig. 7 the profiles of $n_1(z)$ are shown at several values of the undersaturation ϵ. The asymptotic densities at $z \to \pm\infty$ in Fig. 7 are those of the coexisting I and N_2 bulk phases (at the corresponding ϵ). For $\epsilon \to 0$ value $n_1(z)$ in the film approaches the density of thin rods of the bulk triple point N_1 phase, indicated by the dashed line in Fig. 7. However, the undersaturation $\epsilon = 10^{-4}$ is yet too large to be in the asymptotic thick-film regime. The same identification can be made for $n_2(z)$ and $S_\sigma(z)$, and on this basis we conclude that the wetting phenomenon under consideration is complete triple point wetting of the free IN_2 interface by the N_1 phase. The similarity with complete wetting of the IN_2 interface by the N_1 phase in additive thin-thick mixture with $d = 4.0$ is again rather striking, as is clear from Fig. 6, where the thickness of the IN_2 interface for additive rods is indicated by ($\circ$).

Since one expects, for the short-range interactions of interest here, that the thickness of the wetting N_1 film in the IN_2 interface diverges as $t \sim -\xi_{N_1} \ln\epsilon$ for $\epsilon \to 0$[26], the value of the correlation length of the bulk N_1 phase can be extracted, $\xi_{N_1} = 0.49 \pm 0.02$, which is consistent with the earlier determined value from decay of $\rho_\sigma(z,\theta)$ into the bulk N_1 phase.

The analysis of the structural properties of the IN_2 interface can be complemented by studies of the ratio of

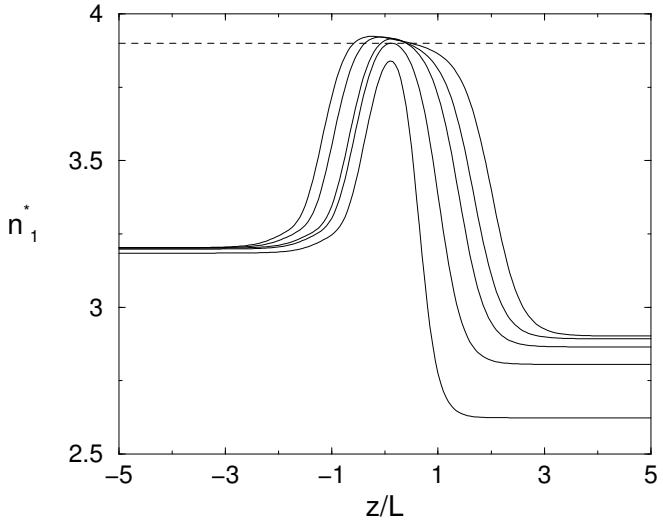

FIG. 7: Density profiles of the thin rods $n_1^*(z)$ in the IN_2 interface for diameter ratio $d = 3.5$ and nonadditivity $\alpha = 0.07$ at triple point undersaturations $\epsilon = 1 - p/p_t = 10^{-2}, 10^{-2.5}, 10^{-3}, 10^{-3.5}, 10^{-4}$. The bulk I/N_2 phase is at $z \to -\infty/\infty$. The dashed line $n_1^* = 3.977$ represents the bulk density of thin rods in the triple point N_1 phase. These profiles indicate the formation of a wetting N_1 film in the IN_2 interface.

surface tensions

$$R(\epsilon) = \frac{\gamma_{IN_2}(\epsilon)}{\lim_{p\downarrow p_t}(\gamma_{IN_1} + \gamma_{N_1N_2})}, \tag{13}$$

as presented in the Inset in Fig. 6. It is clear that upon approach of triple-point coexistence $\lim_{\epsilon\to 0} R(\epsilon) = 1$, which implies a vanishing contact angle. This provides the thermodynamic proof of complete triple-point wetting. The ϵ-dependence of R again reveals that $\epsilon = 10^{-4}$ is too large to be in the asymptotic thick-film regime.

VI. SUMMARY AND DISCUSSION

In this paper we have explored the bulk phase diagrams and the interfacial properties of the nonadditive mixtures of thin and thick hard rods. The nonadditivity was introduced in an attempt to effectively capture some of the effects of soft interactions between them, having in mind mixtures of bare and PEG-coated fd virus particles in aqueous suspension[11]. We showed that the effective hard-core diameter of the unlike interactions, $\frac{1}{2}(D_1 + D_2)(1 + \alpha)$ with D_1 and D_2 the effective diameter of the like interactions, can easily be smaller or larger than the additive case, $\frac{1}{2}(D_1 + D_2)$, by more than a few per cent.

As is illustrated in Fig. 3, a small amount of nonadditivity $\alpha > 0$ can stabilize the high-density nematic-nematic phase coexistence, even if it is only metastable for an additive mixture with the same diameter ratio. However, the experimentally observed lower critical point of the nematic-nematic demixing transition[11] could *not* be reproduced by incorporating nonadditivity into the theory. We suggest, therefore, that further theoretical studies of this system should consider in more detail the impact in particular of a finite bending flexibility, beyond the ground-state approximation[15]. Another issue that needs to be resolved is the (elastic) response of the polymer coat to volume exclusion between the rods, an aspect completely ignored in our analysis.

We find the bulk phase diagrams of nonadditive binary mixtures to show a large similarity with those of the additive mixtures of larger diameter ratio. This is most likely related to the linear dependence of the rod-rod excluded volume on both the diameter ratio d and the nonadditivity α albeit that is it not clear whether there is an exact mapping linking non-additive and additive hard-rod mixtures. We also found that many if not all of the interfacial phenomena that we studied are similar to those of additive mixtures with a larger diameter ratio. Similar to the interfaces between different bulk phases in additive mixtures, the IN_1 and N_1N_2 interfaces are smooth and monotonic, whereas the IN_2 interface exhibits complete wetting by the N_1 phase upon approach of the triple phase coexistence. The complete triple-point wetting scenario was confirmed by (i) the logarithmic divergence of the thickness of the N_1 film with vanishing undersaturation, and (ii) the surface tension ratio $\lim_{\epsilon\to 0} R = 1$. Such a similarity between properties of additive and nonadditive mixtures may represent a significant difficulty to distinguish these in experiments.

Acknowledgments

It is a pleasure to thank Kirstin Purdy, Henk Lekkerkerker, and Seth Fraden for stimulating discussions, and Seth Fraden and Kirstin Purdy for sharing unpublished experimental results with us. This work is part of the research program of the Stichting voor Fundamenteel Onderzoek der Materie (FOM), which is financially supported by the Nederlandse organisatie voor Wetenschappelijk Onderzoek (NWO).

[1] L. Onsager, Ann. N.Y. Acad. Sci. **51**, 627 (1949).
[2] H.H. Wensink and G.J. Vroege, J. Chem. Phys. **119**, 6868 (2003).
[3] A. Speranza and P. Sollich, J. Chem. Phys. **117**, 5421

(2002).
[4] E.M. Kramer and J. Herzfeld, Phys. Rev. E **58**, 5934 (1998).
[5] P. van der Schoot and M.E. Cates, Langmuir **10**, 670 (1994).
[6] G.J. Vroege and H.N.W. Lekkerkerker, Rep. Prog. Phys. **55**, 1241 (1992).
[7] G.J. Vroege and H.N.W. Lekkerkerker, J. Phys. Chem. **97**, 3601 (1993).
[8] E. Grelet and S. Fraden, Phys. Rev. Lett. **90**, 198302 (2003).
[9] R. van Roij and B. Mulder, Europhys. Lett. **34**, 201 (1996).
[10] Z. Dogic and S. Fraden, Phil. Trans. R. Soc. Lond. A **359**, 997 (2001).
[11] K. Purdy et al., cond-mat/0406175.
[12] R. van Roij, B. Mulder and M. Dijkstra, Physica A **261**, 374 (1998).
[13] K. Shundyak and R. van Roij, Phys. Rev. E **68**, 061703 (2003).
[14] S. Varga, A. Galindo, and G. Jackson, Mol. Phys. **101**, 817 (2003).
[15] A. Semenov and A. Subbotin, Polym. Sci. USSR **31**, 2266 (1989).
[16] R. van Roij, to be published.
[17] A. Stroobants, H.N.W. Lekkerkerker, and Th. Odijk, Macromolecules **19**, 2232 (1986).
[18] A. Jusufi, M. Watzlawek, and H. Löwen, Macromolecules **32**, 4470 (1999).
[19] J.F. Joanny, J. Phys. France **49**, 1981 (1988).
[20] S. Fraden, in *Observation, Prediction and Simulation of Phase Transitions in Complex Fluids*, edited by M. Baus *et al.* (Kluwer, Dordrecht, 1995), p. 113.
[21] H.N.W. Lekkerkerker, Ph. Coulon, R. Van Der Haegen, and R. Deblieck, J. Chem. Phys. **80**, 3427 (1984).
[22] R. van Roij and B. Mulder, J. Chem. Phys. **105**, 11237 (1996); J. Chem. Phys. **109**, 1584 (1998).
[23] K. Shundyak and R. van Roij, Phys. Rev. E **69**, 041703 (2004).
[24] K. Shundyak and R. van Roij, J. Phys.: Condens. Matter **13**, 4789 (2001).
[25] K. Shundyak and R. van Roij, Phys. Rev. Lett. **88**, 205501 (2002).
[26] R. Evans, Adv. Phys. **28**, 143 (1979).